METRICA
METRology Institutional CAtalog

ISTITUTO NAZIONALE DI RICERCA METROLOGICA
Repository Istituzionale

# Experimental determination of sensitivity coefficients of some influence parameters in Rockwell B, C, 15N, 30N and 45N

*Original*
Experimental determination of sensitivity coefficients of some influence parameters in Rockwell B, C, 15N, 30N and 45N / Prato, A., Guido, R., Murgia, M., Guerra, A., Rizza, P., Origlia, C., Germak, A.. - In: MEASUREMENT. SENSORS. - ISSN 2665-9174. - 38:(2025). [10.1016/j.measen.2024.101449]

*Availability:*
This version is available at: 11696/87159 since: 2026-03-09T15:28:27Z

*Publisher:*
Elsevier Ltd

*Published*
DOI:10.1016/j.measen.2024.101449

*Terms of use:*

This article is made available under terms and conditions as specified in the corresponding bibliographic description in the repository

*Publisher copyright*

(Article begins on next page)

08 November 2026

Measurement: Sensors 38 (2025) 101449

Contents lists available at ScienceDirect

Measurement: Sensors

journal homepage: www.sciencedirect.com/journal/measurement-sensors

# Experimental determination of sensitivity coefficients of some influence parameters in Rockwell B, C, 15N, 30N and 45N

ARTICLE INFO

*Keywords:*
Rockwell hardness
Uncertainty
Sensitivity coefficient
Monte Carlo method

ABSTRACT

The impact of key variables on hardness measurements, including indenter velocity, geometry, dwell times, forces, and temperature, has been extensively studied in recent decades. The recent adoption of international Rockwell hardness scale definitions has intensified this interest. While these definitions and relevant standards consider parameter ranges, the Rockwell hardness equation lacks explicit incorporation of these variables, requiring an empirical determination of their sensitivity coefficients. This study focuses on the determination of sensitivity coefficients associated with two main influential parameters – the velocity of the final load application and the time interval for the force variation from the preliminary force value to the total force value – across Rockwell B, C, 45N, 30N, and 15N hardness scales at various hardness levels, using a Monte Carlo method and multiple linear regression. The results align with findings in existing literature, enhancing the robustness and reliability of the study.

## 1. Introduction

In hardness measurements, researchers have striven to assess measurement uncertainty by quantifying the impact of various influencing factors [1–7]. This interest has been further increased by the recent adoption of international definitions of Rockwell hardness scales, as provided by the Working Group on Hardness of Consultative Committee for Mass and Related Quantities of the Bureau International des Poids et Mesures, which specify measurement procedures and establish reference values for influencing parameters such as preliminary and total test force, dwell times, indentation velocity, and temperature [8–15]. Although phenomena like creep and other elasto-plastic and dynamic effects can profoundly affect material behaviour, these contributions are not directly considered in the mathematical models of hardness scales, which predominantly rely on geometric factors like indentation depth ($h$ for the Rockwell scale). However, related standards address these effects [16,17]. This study examines two influencing parameters for Rockwell B, C and superficial (45N, 30N and 15N) hardness scales: the total force application velocity and the time interval for force variation. We chose to study these two parameters in depth because their effect on the measurement results can be easily confused since there is a strong correlation between them. Given the challenge of physically decoupling these variables [2], a meticulous experimental design preceded the investigation. Sensitivity coefficients and their uncertainties for each influencing parameter are calculated using a Monte Carlo method applied to multiple linear regression (MLR). Part of this study, related to Rockwell superficial hardness, was already published in Ref. [6]. Comparative analyses with results found in literature are also provided.

## 2. Methods and procedures

### 2.1. Rockwell hardness test cycle

Due to the influence of block material behavior (including creep and elasto-plasticity) and technical considerations regarding machinery dynamics, it is important to comprehend the phases involved in a standardized Rockwell hardness testing cycle. Initially, the indenter approaches the hardness block surface (approach velocity), followed by the application of a preliminary force, $F_0$, during a time interval $t_{pa}$. This force is maintained for a duration, during which an initial depth measurement is taken at time $t_{pd}$. Subsequently, the force is incrementally increased to its total value, $F$, over a time interval $t_{aa}$, divided into two sub-phases: from $F_0$ to $0.8 \bullet F_0$ and then to $F$. The final force is maintained for a time interval $t_{td}$ before rapid reduction to the preliminary force value, $F_0$, over interval $t_{ar}$. This force is maintained until a final depth measurement is taken at time $t_{rd}$, after complete removal of the force. Fig. 1 illustrates this process schematically [8–11].

Understanding the rationale behind each step is intuitive given the testing cycle description: longer maintenance of force relates to creep effects, potentially resulting in lower measured hardness. Conversely, rapid load application may induce hardening phenomena, yielding higher hardness. Similarly, during unloading, an irreversible time-dependent elasto-plastic recovery mechanism occurs. Consequently, steps involving constant load application could be characterized by noise, vibrations, and non-linear behavior.

### 2.2. Experimental plan

This paper investigates the influence of the velocity of final load application ($v_{fa}$) and the time interval for force variation from

https://doi.org/10.1016/j.measen.2024.101449

Available online 19 December 2024

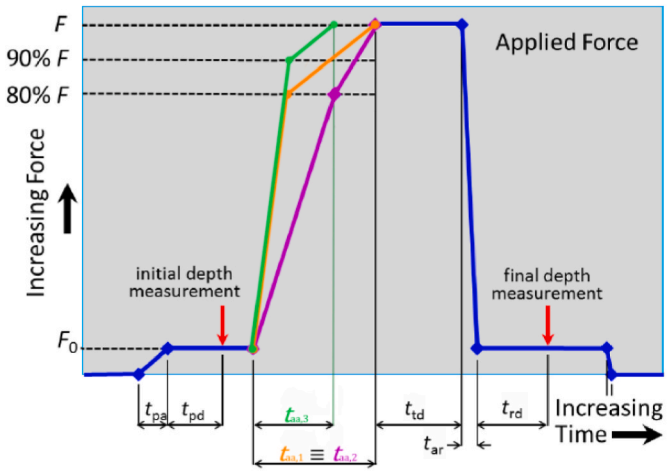


**Fig. 1.** Possible trends in a Rockwell hardness test in a force-time diagram [8–11].

preliminary load to the final load ($t_{aa}$) in Rockwell hardness measurements, particularly due to their association with creep and elasto-plastic effects.

Both, Rockwell hardness scales definition and relevant standards require different ranges for the investigated parameters for the different scales (see Table 1) [8–11,16,17]. Therefore, it becomes crucial to investigate their influence to correct hardness values and evaluate the final uncertainty, in particular for comparison purposes [18].

Based on these ranges of values, experimental plans are designed. A rigorous setup of testing machine parameters is conducted to achieve the desired physical decoupling of velocity-time experimental plans, a task often challenging due to the intrinsic correlation between load application time and velocity. It's established since Ronald Fisher's groundbreaking research in 1926 [19–21] that the design of experiments affects both the outcomes and the level of uncertainty associated with them. Specifically, when there are correlations among independent parameters in a given set, it tends to yield less accurate results and higher uncertainties. Hence, it becomes important to devise an appropriate experimental design that aligns with the desired level of uncertainty. Opting for a full factorial experimental plan, which encompasses a vast array of combinations, is essential when aiming for the lowest possible level of uncertainty.

Given the flexibility of the INRiM Primary Hardness Standard Machine (PHSM), loading cycles with identical application times but differing final velocities can be executed. Three reference blocks spanning low, medium, and high nominal hardness values are selected for each investigated Rockwell hardness scale, i.e., HRB, HRC, HR15N, HR30N, and HR45N, as summarized in Table 2. All blocks are made of steel except for the low and medium blocks for Scale B, which are made of brass.

These blocks are obtained from cylindrical elements through extrusion which are then cut in a section perpendicular to the axis. The hardness values could therefore vary on the face of the block, both in the radial and circumferential directions. To avoid experimental values influenced by local imperfections of the specimen, the measurements are carried out on a curve that varies in both directions (different angles and radii in the polar coordinate system). With the help of a marker, a spiral was drawn on each block, and the hardness tests were carried out on this trace, as evident in Fig. 2.

Experimental plans detailing hardness scales and nominal testing values for $v_{fa}$ and $t_{aa}$, are defined. A total of 27 measurements per scale and block were performed, yielding 81 measurements in total for each investigated scale and 405 measurements in total among all scales. These comprised 3 $t_{aa}$ values × 3 $v_{fa}$ values × 3 repetitions under fixed nominal $v_{fa}$ and $t_{aa}$, summarized in Table 3.

Through these experimental plans, the study investigates parameter variations while holding the other constant, with central values aligning with prescribed nominal values. For example, the experimental plan for Rockwell B scale is shown in Fig. 3.

Sensitivity coefficients and their uncertainties are then determined using a Monte Carlo method applied to multiple linear regression (MLR).

**Table 1**
Reference values prescribed in the definition and in the relevant standards for the velocity of final load application ($v_{fa}$) and the time interval for force variation from preliminary load to the final load ($t_{aa}$) at different Rockwell scales.

| Scale | $v_{fa}$/μm/s | | | $t_{aa}$/s | | |
|---|---|---|---|---|---|---|
| | CCM WGH def. | ISO 6508-1 | ISO 6508-3 | CCM WGH def. | ISO 6508-1 | ISO 6508-3 |
| **B** | – | – | $15 \leq v \leq 40$ | – | $1 \leq t \leq 8$ | $1 \leq t \leq 8$ |
| **C** | 30 | – | $15 \leq v \leq 40$ | $1 \leq t \leq 8$ | $1 \leq t \leq 8$ | $1 \leq t \leq 8$ |
| **45N** | 30 | – | $15 \leq v \leq 40$ | ≤4 | ≤4 | ≤4 |
| **30N** | 30 | - | $15 \leq v \leq 40$ | ≤4 | ≤4 | ≤4 |
| **15N** | 15 | – | $15 \leq v \leq 40$ | ≤4 | ≤4 | ≤4 |

**Table 2**
Nominal hardness of selected blocks at different Rockwell scales.

| Scale | Nominal hardness/HR | | |
|---|---|---|---|
| | Low | Medium | High |
| **B** | 30 | 60 | 90 |
| **C** | 20 | 40 | 60 |
| **45N** | 20 | 40 | 70 |
| **30N** | 40 | 60 | 80 |
| **15N** | 70 | 80 | 90 |

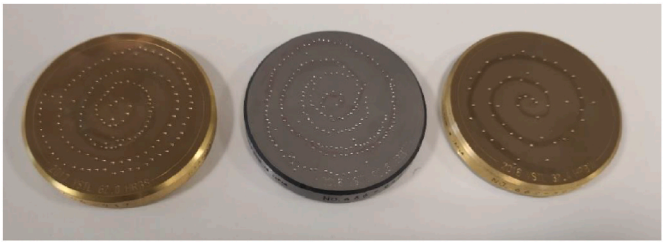

**Fig. 2.** The blocks used for Rockwell B hardness tests. The indentations derived from the hardness tests are visible. The distances between the centres of two adjacent indentations fulfil the requirement of the standard. Additional indentations are subsequently carried out to settle the blocks and the indenter.

### 2.3. INRiM primary hardness standard machine

Measurements are performed with the INRiM Primary Hardness Standard Machine (PHSM). This machine is capable of realizing all Rockwell scales, Vickers scales ranging from HV3 to HV100, and Brinell

**Table 3**
Experimental plan nominal values for the velocity of final load application ($v_{fa}$) and the time interval for force variation from preliminary load to the final load ($t_{aa}$) at different Rockwell scales.

| Scale | Nominal test values for $v_{fa}$/μm/s | | | Nominal test values for $t_{aa}$/s | | |
|---|---|---|---|---|---|---|
| **B** | 20 | 30 | 40 | 5 | 6 | 7 |
| **C** | 20 | 30 | 40 | 4 | 6 | 8 |
| **45N** | 20 | 30 | 40 | 3 | 4 | 5 |
| **30N** | 20 | 30 | 40 | 3 | 4 | 5 |
| **15N** | 10 | 15 | 20 | 3 | 4 | 5 |

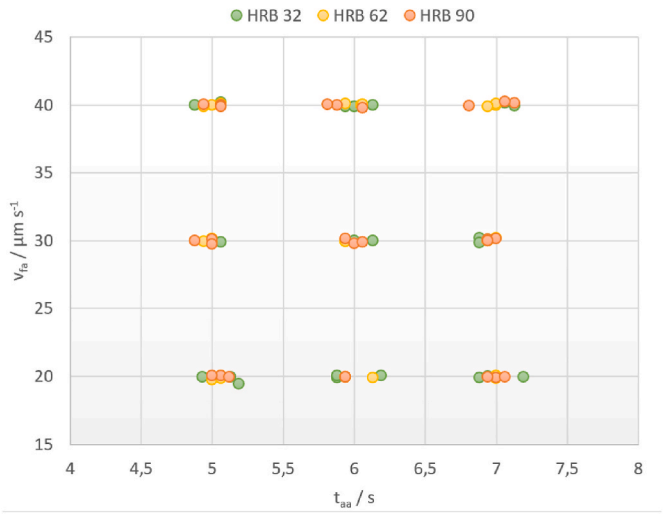


**Fig. 3.** Experimental plan for Rockwell B hardness tests with actual values of parameters under investigation.

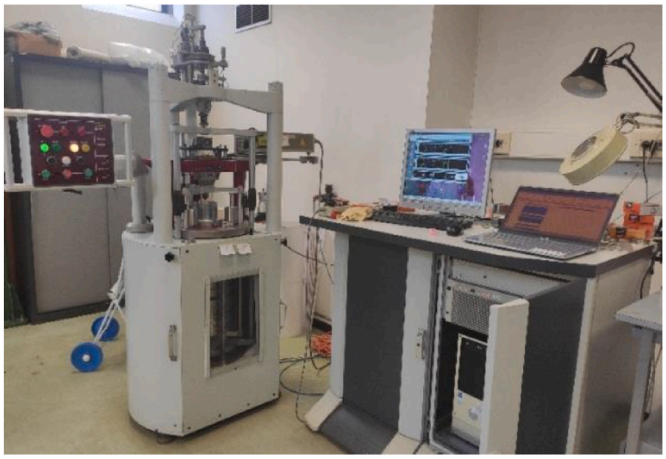

**Fig. 4.** INRiM primary hardness standard machine.

scales from HBW1/5 to HBW2.5/187.5 (see Fig. 4). Technical features and metrological characterization are summarized in detail in Refs. [22–25]. Initially designed and built in the late 1970s, it underwent enhancements in electronic, electro-mechanical, and software control during its second iteration in the early 1990s for NIST (USA). Further improvements were made during its third version for the LFT accredited calibration laboratory, as well as for numerous other NMIs and laboratories in various countries including Brazil, Bulgaria, India, Republic of Korea, USA, China, and Saudi Arabia. The machine comprises a dead weight system for generating test forces and a laser interferometric system for measuring indentation depth. Notable features include high stiffness, an isostatic design, and highly flexible software control for adjusting and measuring key parameters involved in the test cycle, such as times and velocities. Its metrological characteristics enable the realization of hardness scales with exceptional accuracy, setting a benchmark in the field.

### 2.4. Multiple linear regression and uncertainty assessment

A significant challenge in calculating sensitivity coefficients is related to several factors: firstly, inadequate experimental design, resulting in difficulty decoupling parameters and thus attributing specific measurement changes to particular variables. Secondly, even with a successful experimental design, doubts arise regarding sensitivity

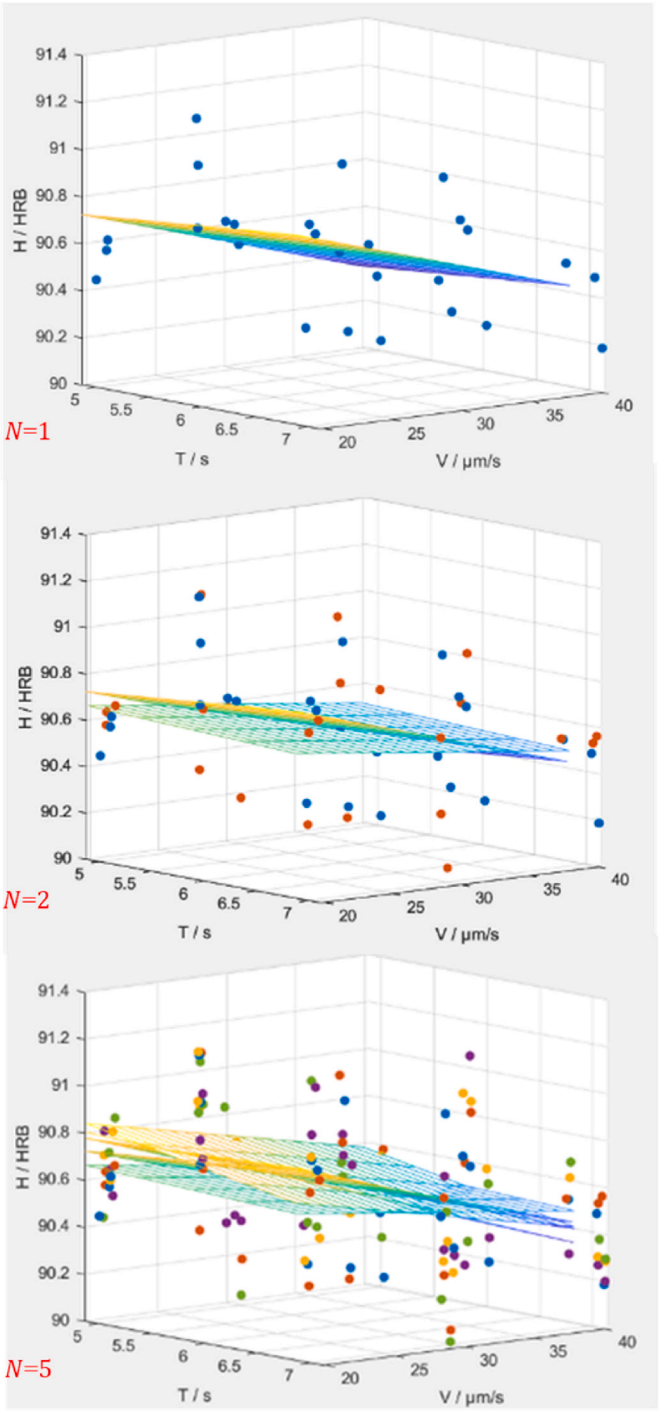


**Fig. 5.** Graphs generated by the MC algorithm for $N_{MC} = 1$, $N_{MC} = 2$ and $N_{MC} = 5$. Example for HRB at high hardness level.

coefficient uncertainty calculation. In hardness measurement, for instance, uncertainty is often directly linked to sensitivity coefficients, while in other cases, sensitivity coefficient uncertainty derives from MLR standard error. However, due to hardness measurement and input variable ($v_{fa}$ and $t_{aa}$) variability, conventional MLR methods may not suffice for sensitivity coefficient evaluation when both input and output variables have uncertainties [6]. For this reason, it is preferable to use a Monte Carlo method applied to MLR.

Suppose that through experimental analysis, a set of $N_{exp}$ measurement conditions is established (27 for each block and scale, in this case). Subsequently, experiments are conducted for each condition.

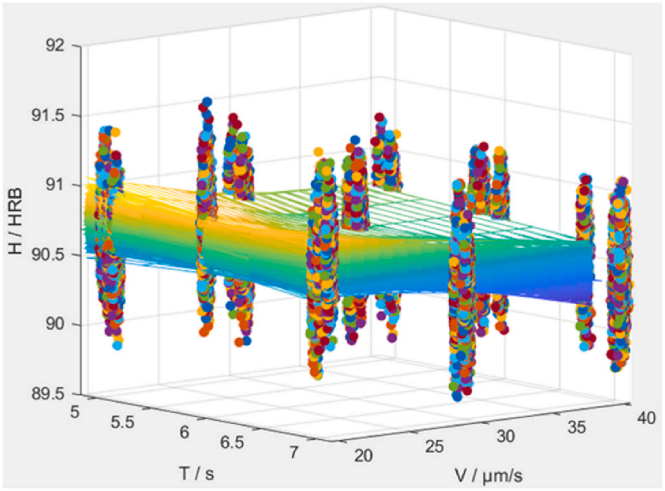


**Fig. 6.** Graphs generated by the MC algorithm for $N_{MC} = 10^6$. Example for HRB at high hardness level.

Measurements include input values $h$, $v_{fa}$, $t_{aa}$ and output values $HR$. Probability density functions (PDFs), such as Normal distribution, are then assigned for each measurement condition to each variable (input and output) based on their uncertainty contributions, e.g. arising from instrumentation (e.g. a standard uncertainties of $5.77 \times 10^{-2}$ s associated with $t_{aa}$ and a standard uncertainties of 0.1155 µm $s^{-1}$ associated with $v_{fa}$) or declared CMC for output variables (e.g. in INRiM case, expanded uncertainties of 0.4 HR for B scale and or 0.3 HR for C, 45N, 30N and 15N scales). Using a Monte Carlo (MC) method, input and output variables are then sampled from their respective PDFs, and a MLR is performed. Given the number of parameters, for a first-order model, a regression plane is generated from each sampling, yielding a function in the form of a linear equation

$$HR = \mathrm{N} - \frac{h}{\mathrm{S}} + c_{v_{fa},i} v_{fa} + c_{t_{aa},i} t_{aa}. \quad (1)$$

where $HR$ is the scalar hardness output, N and S are constants according to the relevant Rockwell hardness scale, $h$ is the indentation depth, and the $c_i$ are the sensitivity coefficients at the $i$-th MC iteration (sampling) associated with $v_{fa}$ and $t_{aa}$ which serve as additional input variables. For each $i$-th MC iteration, multiple linear regression (MLR) outputs are $c_{v_{fa},i}$ and $c_{t_{aa},i}$ sensitivity coefficients together with standard uncertainty from ordinary least squares (OLS), $u_{OLS}(c_i)$. At the end of the MC iteration, $N_{MC}$ iterations and regression planes, typically in the order of $10^6$ to $10^7$ as recommended in previous studies [6], are found. These regression planes are used to find the mean values of $c_{v_{fa}}$ and $c_{t_{aa}}$ ($c$, generally speaking) with associated standard deviations $u_{MC}(c)$, as illustrated in (2) and (3).

$$c = \frac{1}{N_{MC}} \sum_{i=1}^{N_{MC}} c_i \quad (2)$$

$$u_{MC}(c) = \sqrt{\frac{\sum_{i=1}^{N_{MC}} (c_i - c)^2}{N_{MC}(N_{MC} - 1)}} \quad (3)$$

The total standard uncertainty of sensitivity coefficients is then determined by summing the squares of $u_{MC}(c)$ and $u_{OLS}(c)$, according to

$$u(c) = \sqrt{u_{MC}(c)^2 + u_{OLS}(c)^2}. \quad (4)$$

where $u_{OLS}(c)$ is the mean standard uncertainty from the $N_{MC}$ OLS given by

$$u_{OLS}(c) = \frac{1}{N_{MC}} \sum_{i=1}^{N_{MC}} u_{OLS}(c_i). \quad (5)$$

Expended uncertainty $U(c)$ is then determined by multiplying standard uncertainty $u(c)$ by 2.

As sensitivity coefficients are derived experimentally, their uncertainties must be accounted for using the law of uncertainty propagation. Further details on how considering the uncertainty of each sensitivity coefficient in the hardness model can be found in previous works [18].

## 3. Results and discussion

In the proposed scenario, the Monte Carlo (MC) method is employed, sampling data from normal distributions obtained from experimental results. A Monte Carlo analysis requires that $N_{MC}$ iterations be completed, and to set up an analysis with this method it is necessary to estimate the value of this $N_{MC}$. A large number of iterations makes it possible to reduce the value of the uncertainty components $u_{MC}(c)$ and $u_{OLS}(c)$, since both are proportional to $1/N_{MC}$. Consequently, the value of $u(c)$ is also be reduced. On the other hand, a high $N_{MC}$ implies very long program execution times, and beyond a certain value of $N_{MC}$, the uncertainty components do not decrease sufficiently to justify such long times. It is therefore necessary to estimate a high enough number of iterations to reduce the uncertainty components but not to require exaggerated times. For this reason, in this work, $N_{MC} = 10^6$ is chosen. Subsequently, the MC method for MLR is executed using a MATLAB script.

For $N_{MC} = 1$ the algorithm will generate 27 points from the 27 experimental ones, as shown in Fig. 5. In addition to this, the algorithm performs a multiple linear regression, which can be visualized with a plane in hardness-time-velocity space. This is represented as a grid whose colour varies according to the hardness value, and is also shown on the same diagram.

For $N_{MC} = 2$, additional 27 points are generated independently of the previous ones, and thus the equation of a new plane in the hardness-time-velocity space is calculated. Both the new points and the new plane are displayed on the same graph as the previous ones, so that they are all displayed together.

These steps are re-executed for subsequent iterations, firstly generating new points, then performing a new regression and obtaining a new plane, and finally returning the new points to the same graph. As an example, Fig. 5 also shows the $N_{MC} = 5$ case.

For a high number of iterations, thus for $N_{MC} = 10^6$, the space starts filling with overlapping points and closer planes. The resulting graph is shown in Fig. 6.

By computing calculations described in the previous Section, sensitivity coefficients of $c_{v_{fa}}$ and $c_{t_{aa}}$ with the associated expanded uncertainty are obtained. These are summarized in the following Table 4 for

**Table 4**
Sensitivity coefficients of $c_{v_{fa}}$ and $c_{t_{aa}}$ and their 95 % expanded uncertainties, derived from Monte Carlo multiple linear regression analysis. To simplify notation, HR represents HRB, HRC, HR45N, HR30N, and HR15N according to the relevant scale.

| Scale | $c_{v_{fa}}$/HR s µm$^{-1}$ | | | $c_{t_{aa}}$/HR s$^{-1}$ | | |
|---|---|---|---|---|---|---|
| | Low | Medium | High | Low | Medium | High |
| **B** | −0.022 ± 0.031 | 0.007 ± 0.024 | −0.015 ± 0.010 | −0.051 ± 0.307 | −0.140 ± 0.246 | −0,017 ± 0.102 |
| **C** | −0.020 ± 0,100 | 0,000 ± 0.100 | 0,030 ± 0.080 | 0.0043 ± 0.0197 | 0.003 ± 0.017 | −0.017 ± 0.015 |
| **45N** | −0.003 ± 0.034 | −0.006 ± 0.021 | −0.005 ± 0.014 | 0.010 ± 0.26 | −0.0143 ± 0.244 | 0.009 ± 0.215 |
| **30N** | −0.004 ± 0.010 | −0.015 ± 0.045 | −0.005 ± 0.025 | 0.044 ± 0.271 | −0.001 ± 0.270 | 0.0044 ± 0.213 |
| **15N** | −0.006 ± 0.032 | −0.029 ± 0.047 | −0.022 ± 0.012 | 0.000 ± 0.140 | 0.022 ± 0.211 | 0.009 ± 0.048 |

all blocks and scales. Data are reported with three decimals to amplify the effect, despite the third digit is usually neglected in hardness measurements.

In general terms, sensitivity coefficients are very small compared to their expanded uncertainty. In addition, it is found that $u_{MC}(c)$ is three order of magnitude lower than $u_{OLS}(c)$, with this huge number of iterations $N_{MC} = 10^6$. In the future, it is worth investigating the influence of the number of iterations on the accuracy and precision of results and the impact and the efficacy of the Monte Carlo method compared to traditional data analysis which usually neglects uncertainty of input and output linear regression model variables.

Comparative analysis with data existing literature, when available, reveals a good agreement, despite different hardness machines and boundary conditions [1,5,7,26,27].

However, it is important to underline that in most of the works possible correlations between these two parameters are usually disregarded and uncertainty of sensitivity coefficients is absent. Also, even when uncertainty details of sensitivity coefficients are provided, a consistent methodology for determining such uncertainty contributions remains elusive. This discrepancy extends to whether uncertainties are solely based on standard uncertainty from ordinary least squares (OLS) for linear regression or mirror the uncertainty of hardness measurements.

Moreover, when hardness is measured and its uncertainty calculated, propagation of sensitivity coefficients standard uncertainty is generally lacking, despite potential significance on the final results, as shown in Ref. [18].

## 4. Conclusions

This paper delves into investigating the impact of the velocity of final load application and the time interval for force variation from preliminary test force to final force on Rockwell B, C, 45N, 30N and 15N hardness measurements. Measurements are performed on three different blocks with increased hardness and with a suitable experimental plan in order to decouple the two parameters which are potentially strongly correlated. The values of these parameters fall within the ranges coming from the definitions and the relevant standards. Sensitivity coefficients and associated uncertainties are derived using a Monte Carlo method for multiple linear regression (MLR), starting from the uncertainties of the input and output model variables. A total of $10^6$ iterations are computed and, at the end, the mean value of the sensitivity coefficients and their uncertainties are evaluated. The latter are evaluated by summing the square of the sensitivity coefficients standard deviation obtained from the Monte Carlo iterations and the mean uncertainty obtained from the ordinary least squares method employed in the regression analysis. The estimated sensitivity coefficients generally are in agreement with those reported in the literature. Uncertainties associated with sensitivity coefficients are pivotal in assessing the significance of a given sensitivity coefficient and must be considered, if substantial, in the combined standard uncertainty of the hardness measurement model, particularly when additional variables are incorporated into the measurement mathematical model, as discussed in prior literature.

## Funding statement

This research did not receive any specific grant from funding agencies in the public, commercial, or not-for-profit sectors.

## References

[1] S. Low, R. Machado, Determination of test cycle sensitivity coefficients for the Rockwell HR45N hardness scale, J. Phys.: Conf. Ser. 1065 (2018) 062008.
[2] G. Barbato, S. Desogus, A. Germak, Experimental analysis on the influence quantities in the Rockwell C hardness test, in: Proc. Int. Symposium on Advances in Hardness Measurement, HARDMEKO, 1998.
[3] G. Barbato, M. Galetto, A. Germak, F. Mazzoleni, Influence of the indenter shape in Rockwell hardness test, Proc. HARDMEKO 98 (1998) 21–23.
[4] Y. Tanaka, K. Hattori, M. Yoshioka, Determining the sensitivity coefficients of factors contributing to Rockwell hardness for uncertainty evaluation, Measurement 227 (2024).
[5] L. Brice, S. Low, R. Jiggetts, Determination of sensitivity coefficients for Rockwell hardness scales HR15N, HR30N, and HRA, in: 18th IMEKO WORLD CONGRESS Metrology for a Sustainable Development, 2006.
[6] P. Rizza, M. Murgia, A. Prato, C. Origlia, A. Germak, Determination of sensitivity coefficients and their uncertainties in Rockwell hardness measurement: a Monte Carlo method for multiple linear regression, Metrologia 60 (1) (2022).
[7] European Association of National Metrology, Guidelines on the estimation of uncertainty in hardness measurements, in: EURAMET cg 16, 2011, Version 2.0.
[8] BIPM – Consultative Committee for Mass and Related Quantities – Working Group on Hardness (CCM-WGH), Rockwell Hardness HR15N Scale Definition, 2021.
[9] BIPM – Consultative Committee for Mass and Related Quantities – Working Group on Hardness (CCM-WGH), Rockwell Hardness HR30N Scale Definition, 2021.
[10] BIPM – Consultative Committee for Mass and Related Quantities – Working Group on Hardness (CCM-WGH), Rockwell Hardness HR45N Scale Definition, 2021.
[11] BIPM – Consultative Committee for Mass and Related Quantities – Working Group on Hardness (CCM-WGH), Rockwell Hardness HRC Scale Definition, 2021.
[12] S. Low, A. Germak, A. Knott, R. Machado, J. Song, Developing definitions of conventional hardness tests for use by National Metrology Institutes, Measurement: Sensors 18 (2021) 100096.
[13] A. Germak, K. Herrmann, S. Low, Traceability in hardness measurements: from the definition to industry, Metrologia 47 (2010) S59.
[14] J.F. Song, S. Low, D. Pitchure, A. Germak, S. Desogus, T. Polzin, H.Q. Yang, H. Ishida, G. Barbato, Establishing a world-wide unified Rockwell hardness scale with metrological traceability, Metrologia 34 (1997) 331.
[15] S. Low, A. Germak, K. Herrmann, Traceability of industrial Rockwell, Brinell, Vickers and knoop hardness measurements, in: IMEKO 2010 TC3, TC5 and TC22 Conf.: Metrology in Modern Context, 2010, pp. 193–196.
[16] ISO, 6508-1, Metallic Materials—Rockwell Hardness Test – Part 1: Test Method, International Organization for Standardization, Geneva, 2016.
[17] ISO 6508-3, Metallic Materials – Rockwell Hardness Test – Part 3: Calibration of Reference Blocks, 2015.
[18] P. Rizza, A. Prato, R. Machado, A. Germak, The role of influence coefficients in hardness measurements: a case study in Rockwell hardness measurements, Measurement 213 (2023) 112713.
[19] R. Fisher, The arrangement of field experiments, Journal of the Ministry of Agriculture of Great Britain 33 (1926) 503–513.
[20] A. Prato, D. Borgiattino, F. Mazzoleni, A. Facello, A. Germak, Theoretical insights on the influence of the experimental plan in the calibration of multicomponent force and moment transducers, Measurement: Sensors 18 (2021).
[21] A. Prato, D. Borgiattino, A. Facello, F. Mazzoleni, A. Germak, Calibration of multicomponent force and moment transducers using uniaxial force standard machines integrated with tilted plates, Meas. Sci. Technol. 33 (2022) 095023.
[22] G. Barbato, S. Desogus, R. Levi, Design and performance of a dead-weight standard Rockwell hardness testing machine, J. Test. Eval. 6 (1978) 276–279.
[23] A. Germak, A. Liguori, C. Origlia, Experience in the metrological characterization of primary hardness standard machines, in: Proc. Of HARDMEKO, 2007.
[24] G. Barbato, S. Desogus, R. Levi, Design studies and characteristics description of the standard dead-weight hardness tester of the Instituto di Metrologia G. Colonnetti (IMGC), Hardness Test. Theor. Pract. (1978) 97–103.
[25] A. Schiavi, C. Origlia, A. Germak, A. Prato, G. Genta, Indentation modulus, indentation work and creep of metals and alloys at the macro-scale level: experimental insights into the use of a primary Vickers hardness standard machine, Materials 14 (11) (2021) 2912.
[26] K. Herrmann, M. Zhamanbalin, Final report on COMMET Rockwell PTB/KazlnMetr comparison, Metrologia 46 (2009) 07001.
[27] Website of National Physical Laboratory (NPL), Rockwell hardness sensitivity coefficients HRB, https://www.npl.co.uk/getattachment/products-services/Advanced-materials/Hardness-testing/rockwell_hardness_co_hrb.pdf?lang=en-GB.

Andrea Prato[a,*], Roberto Guido[b], Marcello Murgia[b], Alberto Guerra[b], Pierluigi Rizza[b], Claudio Origlia[a], Alessandro Germak[a]
[a] *INRiM – Istituto Nazionale di Ricerca Metrologica, Torino, Italy*
[b] *Politecnico di Torino, Torino, Italy*

[*] Corresponding author.
*E-mail addresses:* a.prato@inrim.it (A. Prato), roberto.guido@studenti.polito.it (R. Guido), marcello.murgia@studenti.polito.it (M. Murgia), alberto.guerra@studenti.polito.it (A. Guerra), pierluigi.rizza@polito.it (P. Rizza), c.origlia@inrim.it (C. Origlia), a.germak@inrim.it (A. Germak).